Critical intermediate phase and phase transitions in a triangular-lattice three-spin interaction model: Level-spectroscopy approach

2008 J. Phys. A: Math. Theor. 41 375001

(http://iopscience.iop.org/1751-8121/41/37/375001)

IOP PUBLISHING JOURNAL OF PHYSICS A: MATHEMATICAL AND THEORETICAL

J. Phys. A: Math. Theor. **41** (2008) 375001 (21pp) doi:10.1088/1751-8113/41/37/375001

Critical intermediate phase and phase transitions in a triangular-lattice three-spin interaction model: Level-spectroscopy approach

Hiromi Otsuka[1] **and Kiyohide Nomura**[2]

[1] Department of Physics, Tokyo Metropolitan University, Tokyo 192-0397, Japan
[2] Department of Physics, Kyushu University, Fukuoka 812-8581, Japan

E-mail: otsuka@phys.metro-u.ac.jp

Received 11 April 2008, in final form 15 July 2008
Published 7 August 2008
Online at stacks.iop.org/JPhysA/41/375001

Abstract

We investigate infinite-order phase transitions like the Berezinskii–Kosterlitz–Thouless transition observed in a triangular-lattice three-spin interaction model. Based on a field theoretical description and the operator-production-expansion technique, we perform the renormalization-group analysis, and then clarify properties of marginal operators near the phase transition points. The results are utilized to establish criteria to determine the transition points and some universal relations among excitation levels to characterize the transitions. We verify these predictions via the numerical analysis on eigenvalue structures of the transfer matrix. Also, we discuss an enhancement of symmetry at the end points of a critical intermediate phase in connection with a transition observed in the ground state of the bilinear-biquadratic spin-1 chain.

PACS numbers: 64.60.−i, 05.50.+q, 05.70.Jk

1. Introduction

Phase transitions and critical phenomena observed in classical spin systems have been investigated for a long time. Their theoretical treatments including numerical ones have revealed a variety of features, and also have been offering the interfaces to understand real materials. At the same time, the universality observed in phase transitions is one of the most important concepts. For the two-dimensional (2D) critical systems, it is pronouncedly expressed in terms of the conformal symmetry being possessed by relevant effective field theories. The central charge c is the widely-known theoretical parameter [1]. In the case $c < 1$, it appears to almost characterize a universality class, i.e., a possible set of critical exponents [2]: the discrete systems such as the Ising and the three-state Potts ferromagnets show the second-order transitions whose universality classes are given by the conformal

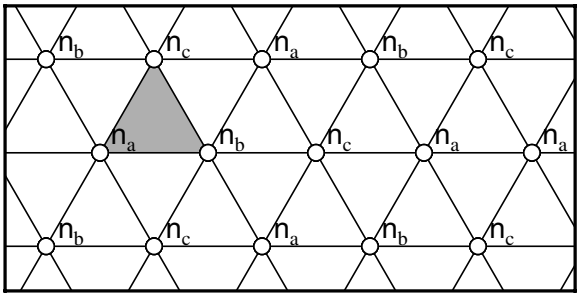

Figure 1. The triangular lattice Λ and the sublattice dependent numbers (n_a, n_b, n_c) (see the text). The shaded area exhibits the elementary plaquette of Λ.

symmetries with the rational values of c. On the other hand, in the case $c \geqslant 1$, there still exist considerable efforts to understand the universalities of phase transitions.

It is widely known that the systems with strong frustrations sometimes exhibit the residual entropies and the critical ground states with $c \geqslant 1$. Those of the triangular-lattice Ising [3–6] and the square-lattice three-state Potts antiferromagnets [7, 8] are the typical ones with $c = 1$. Further, the Kagomé-lattice three-state Potts [9, 10] and the square-lattice four-state Potts vertex antiferromagnets [11, 12] were clarified to possess the ground states with $c = 2$ and $c = 3$, respectively [13, 14]. In addition, the dimer, the loop gas, and the coloring models (some of them can be related to the spin models) are other examples to show the criticality with $c \geqslant 1$ [15]. Also, the frustration effects can increase the central charge of the finite-temperature criticality as observed in the 2D fully frustrated XY model [16]. So they have been gathering great attentions for long time both theoretically and experimentally.

On another front, multispin interactions appear to include an effect to enhance the central charge: the exactly solved Baxter–Wu model consisting of the three Ising-spin product interaction is the most basic one [17]; it shows the second-order transition whose universality is the same as that of the four-state Potts ferromagnet [18]. The Ising and the four-state Potts criticalities are of $c = 1/2$ and $c = 1$, respectively. Therefore, the multispin interactions are expected as an another source to bring about larger values of c, although they have not been argued frequently in this context.

In this paper, we investigate the three-spin interaction model (TSIM) introduced a long time ago by Alcaraz *et al* [19, 20]. Suppose that $\langle k, l, m\rangle$ denotes three sites at the corners of each elementary plaquette (see the shaded area in figure 1) of the triangular lattice Λ consisting of interpenetrating three sublattices Λ_a, Λ_b and Λ_c, then the following reduced Hamiltonian expresses a class of TSIM:

$$\mathcal{H} = -\frac{J}{k_B T} \sum_{\langle k,l,m\rangle} \cos(\varphi_k + \varphi_l + \varphi_m). \tag{1}$$

One model parameter, the temperature T, will be measured in units of J/k_B. The angle variables $\varphi_k = 2\pi n_k/p$ ($n_k \in [0, p-1]$) are located on sites, and define the $\mathbb{Z}_p$ clock variables [21] (the Baxter–Wu model is contained as its special case of $p = 2$). As we shall take a quick look at them in section 2, the most intriguing ones are the properties of an critical intermediate phase theoretically expected for $p \geqslant 4$, and its instabilities to the ordered and the disordered phases. Alcaraz *et al* derived the vector Coulomb gas (CG) representation of the model [20]. Especially, they provided the renormalization-group (RG) analysis based on its similarity to the triangular-lattice defect-mediated melting phenomenon which is known as

the Kosterlitz–Thouless–Halperin–Nelson–Young (KTHNY) theory [22–26]. In the previous paper, we also argued the effective description of TSIM based on the symmetry properties and the so-called ideal-state graph concept by Kondev and Henley [13, 14, 27]; and then introduced the vector dual sine-Gordon Lagrangian density [28]. Since its criticality is of c equal to the number of components of the vector field, $c = 2$ was theoretically expected. We performed the numerical calculations to confirm this and further the properties of the low-energy excitations. However, a detailed analysis of the model on and around the transition points has not been done yet. Here, based on the effective field theory, we shall first perform the RG analysis, and derive the RG equations to describe the transitions to the ordered and the disordered phases. In both cases, we discuss a mixing of marginal operators along a separatrix embedded in the RG-flow diagram because the same argument was done for the sine-Gordon model [29], and its importance has been widely recognized in the discussions of the Berezinskii–Kosterlitz–Thouless (BKT) transitions [22, 30, 31] (for applications to classical systems, see [32–35]). We then clarify excitation spectra characteristic to the phase transitions observed. For these purposes, we shall utilize some formulae which require the so-called conformal field theory (CFT) data such as the scaling dimensions and the operator-product-expansion (OPE) coefficients. Therefore, we provide detailed explanations of the OPE calculations among local density operators in our field theory [36].

The organization of this paper is as follows. In section 2, according to our previous research, we shall explain our Lagrangian density to effectively describe the low-energy and the long-distance behavior of TSIM. The calculations of OPE coefficients necessary for the CFT technology, the RG analysis of phase transitions, and the conformal perturbation calculations of excitation spectra up to the one-loop order are performed there. In section 3, based on the analysis in section 2, we shall explain our numerical calculation procedure (the so-called level-crossing conditions) to determine the transition points. We perform numerical diagonalization calculations of the transfer matrix, and then provide their estimates. Further, to serve a reliability, we check some universal relations among excitation levels observed in finite-size systems—in short, we shall perform the level-spectroscopy analysis of TSIM [29]. The section 4 is devoted to discussions and summary of the present investigation. An enhancement of symmetry at the transition points will be pointed out; we shall discuss its connection with a 1D quantum spin system. For readers' convenience, we shall provide two appendices: in appendix A, we summarize the properties of the critical fixed point of our model which include the conformal invariance as well as OPE's among basic operators. In appendix B, based on appendix A, we provide details in the derivations of some useful relations; these will contribute directly to the analysis of the critical phenomena observed in the present model.

2. Theory

2.1. Vector dual sine-Gordon model

Since the symmetry property is the key to understand the criticality and the phase transitions, we shall begin with its description. Adding to the translations and the space inversions, the model is invariant under the global spin rotations

$$\varphi_k \to \varphi_k + \sum_{\rho=\mathrm{a,b,c}} \sum_{l\in\Lambda_\rho} \frac{2\pi n_\rho}{p} \delta_{k,l} \tag{2}$$

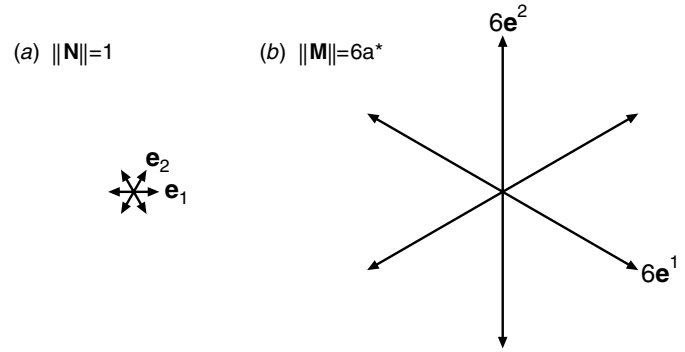

Figure 2. The schematic representation of the vector charges in the Lagrangian density $\mathcal{L}$: (*a*) the magnetic vector charges in $\mathcal{L}_2$ (equation (13)) which represent the discontinuities of Φ. (*b*) The electric vector charges in $\mathcal{L}_1$ (equation (12)) (the $p = 6$ case) which bring about the phase locking potential with the p^2 minima.

with sublattice dependent integers (see figure 1) satisfying the condition $n_a + n_b + n_c = 0 \,(\mathrm{mod}\, p)$ [20]. This symmetry operation—we denote as (n_a, n_b, n_c)—can be generated from two of the following three fundamental operations:

$$\hat{R}_a : (1, p-1, 0),\ \hat{R}_b : (0, 1, p-1) \text{ and } \hat{R}_c : (p-1, 0, 1). \tag{3}$$

Thus, it is referred to as the $\mathbb{Z}_p \times \mathbb{Z}_p$ symmetry. They satisfy some important relations, e.g., $\hat{R}_a^p = \hat{R}_c \hat{R}_b \hat{R}_a = \hat{1}$. Based on these properties, we introduced the vector dual sine-Gordon model in the 2D Euclidean space [28]. Writing the Cartesian components of the position vector $\mathbf{x}$ in the space as (x, y) (see figure 1), then it is defined by the Lagrangian density $\mathcal{L} = \mathcal{L}_0 + \mathcal{L}_1 + \mathcal{L}_2$ with

$$\mathcal{L}_0 = \frac{K}{4\pi} \sum_{i=x,y} \|\partial_i \mathbf{\Phi}(\mathbf{x})\|^2, \tag{4}$$

$$\mathcal{L}_1 = \frac{y_p}{2\pi a^2} \sum_{\|\mathbf{M}\|=pa^*} :\mathrm{e}^{\mathrm{i}\mathbf{M}\cdot\mathbf{\Phi}(\mathbf{x})}:, \tag{5}$$

$$\mathcal{L}_2 = \frac{y_1}{2\pi a^2} \sum_{\|\mathbf{N}\|=1} :\mathrm{e}^{\mathrm{i}\mathbf{N}\cdot\mathbf{\Theta}(\mathbf{x})}:. \tag{6}$$

The symbol ‘: :’ denotes the normal ordering and means the subtraction of possible contractions of fields between them. We shall employ the same definitions of the fields and the vector charges as those in our previous paper: $\mathbf{\Theta}$ is the dual field to $\mathbf{\Phi}$ and is related as $\mathrm{i}K\partial_i \mathbf{\Phi} = \epsilon_{ij}\partial_j \mathbf{\Theta}$ (ϵ_{ij} is the antisymmetric tensor). In figure 2 of [28], we explained the so-called repeat lattice $\mathcal{R}$ representing the periodicity of $\mathbf{\Phi}$ [13, 14]. Using its frame as the Cartesian coordinate, the primitive vectors of $\mathcal{R}$ are given by

$$\mathbf{e}_1 = (1, 0) \qquad \text{and} \qquad \mathbf{e}_2 = \left(\frac{1}{2}, \frac{\sqrt{3}}{2}\right). \tag{7}$$

Also, the primitive vectors of the reciprocal lattice $\mathcal{R}^*$ are given by

$$\mathbf{e}^1 = \left(1, \frac{-1}{\sqrt{3}}\right) \qquad \text{and} \qquad \mathbf{e}^2 = \left(0, \frac{2}{\sqrt{3}}\right). \tag{8}$$

The magnetic (electric) vector charge $\mathbf{N}$ ($\mathbf{M}$) is quantized in $\mathcal{R}$ ($\mathcal{R}^*$) whose contravariant (covariant) element is expressed as $n^\alpha \equiv \mathbf{e}^\alpha \cdot \mathbf{N}$ ($m_\alpha \equiv \mathbf{e}_\alpha \cdot \mathbf{M}$), and satisfies the condition n^α (m_α) $\in \mathbb{Z}$. Using these vectors, the periodicities of the fields are given by $\mathbf{\Phi} \equiv \mathbf{\Phi} + 2\pi\mathbf{N}$ and $\mathbf{\Theta} \equiv \mathbf{\Theta} + 2\pi\mathbf{M}$. The metric tensors for $\mathcal{R}$ and $\mathcal{R}^*$ are defined by $g_{\alpha\beta} = \mathbf{e}_\alpha \cdot \mathbf{e}_\beta$ and $g^{\alpha\beta} = \mathbf{e}^\alpha \cdot \mathbf{e}^\beta$, respectively. They satisfy the condition $g_{\alpha\gamma} g^{\gamma\beta} = \delta_\alpha^\beta$ because of the duality relation $\mathbf{e}_\alpha \cdot \mathbf{e}^\beta = \delta_\alpha^\beta$. A small calculation using equations (7) and (8) yields their explicit forms

$$g_{\alpha\beta} = \begin{pmatrix} 1 & \frac{1}{2} \\ \frac{1}{2} & 1 \end{pmatrix} \qquad \text{and} \qquad g^{\alpha\beta} = \begin{pmatrix} \frac{4}{3} & -\frac{2}{3} \\ -\frac{2}{3} & \frac{4}{3} \end{pmatrix}. \tag{9}$$

The squared norm of, say, $\mathbf{M}$ is given by $\|\mathbf{M}\|^2 = m_\alpha m^\alpha$ ($m^\alpha = g^{\alpha\beta} m_\beta$). In equation (5), the lattice constant of $\mathcal{R}^*$ is denoted as a^* ($=\sqrt{g^{11}}$).[3]

The action $S_0 \equiv \int \mathrm{d}^2x \mathcal{L}_0$ represents an interface model consisting of two kinds of massless scalar fields [13, 14]. Using the elements of $\mathbf{\Phi}$, it is rewritten as

$$S_0 = \int \mathrm{d}^2x \frac{K}{2\pi} \partial_i \phi_\alpha(\mathbf{x}) \partial_i \phi^\alpha(\mathbf{x}), \tag{10}$$

where $\sqrt{2}\phi^\alpha \equiv \mathbf{e}^\alpha \cdot \mathbf{\Phi}$ ($\phi_\alpha = g_{\alpha\beta}\phi^\beta$) (the element of $\mathbf{\Theta}$ is also defined by $\sqrt{2}\theta_\alpha \equiv \mathbf{e}_\alpha \cdot \mathbf{\Theta}$ ($\theta^\alpha = g^{\alpha\beta}\theta_\beta$)). The factor $\sqrt{2}$ is for convenience. Then, the two-point function exhibits the logarithmic behavior

$$\langle \phi^\alpha(\mathbf{x}) \phi^\beta(\mathbf{0}) \rangle_0 = -\frac{1}{4K} g^{\alpha\beta} \ln \left(\frac{r}{a} \right)^2, \tag{11}$$

where r and a are the distance between $\mathbf{x}$ and $\mathbf{0}$ on the basal 2D space and the ultraviolet (UV) cutoff constant, respectively. $\langle \cdots \rangle_0$ means the average respect to the free part S_0. This implies that the fields themselves cannot represent physical quantities. However, as we summarize in appendix A, the current and the vertex operators defined by them are the scaling operators, and represent physical quantities. Since the system defined by S_0 is critical, and possesses the conformal invariance with $c = 2$, the interface model is in a roughening phase if $\mathcal{L}_{1,2}$ are both irrelevant.

The phase locking potential $\mathcal{L}_1$ consists of the six terms with the following electric vector charges (see figure 2(b)):

$$\pm p\,\mathbf{e}^1, \pm p\,\mathbf{e}^2, \text{ and } \pm p(\mathbf{e}^1 + \mathbf{e}^2), \tag{12}$$

whose lengths are all pa^*. In the unit cell of $\mathcal{R}$, it produces the p^2 potential minima which form the triangular lattice as $\mathbf{\Phi}_{\mathrm{lock}} \equiv 2\pi l^\alpha \mathbf{e}_\alpha / p$ with $l^\alpha \in [0, p-1]$ (see figure 1 in [28]), and each of which corresponds to one of the p^2-degenerate states. From the formula, equation (B.3), the RG eigenvalue of $\mathcal{L}_1$ is given by $2 - 2p^2/3K$ on the Gaussian fixed point S_0, so it becomes relevant for $K > p^2/3$. Since the Gaussian coupling K stands for the stiffness of the interface, it is roughly proportional to the inverse temperature. Therefore, $\mathcal{L}_1$ can stabilize the flat phase with the long-range order at low temperature.

Another potential $\mathcal{L}_2$ is defined in term of the dual field $\mathbf{\Theta}$. The vertex operator $\mathrm{e}^{\mathrm{i}\mathbf{N}\cdot\mathbf{\Theta}}$ creates a discontinuity of $\mathbf{\Phi}$ by amount of $2\pi\mathbf{N}$ around the point $\mathbf{x}$. This topological defect is necessary to describe the disordered phase at high temperature. According to the RG sense,

[3] There are three 2D spaces: (i) the basal 2D space of Λ. Since the Cartesian components can be used for the position vector $\mathbf{x}$, we employ the alphabetical subscripts, i, j, to specify them. (ii) The 2D space in which $\mathcal{R}$ is embedded and (iii) its dual space in which $\mathcal{R}^*$ is embedded. Like the case of the crystallography, since we have employed the nonorthogonal primitive vectors, equation (7), for the 2D space to which $\mathbf{\Phi}$ belongs, it is necessary to introduce the dual space spanned by equation (8). In this case, it is convenient to express the vectors as the covariant/contravariant elements; we thus use the Greek alphabets, α, β, γ, as the subscript/superscript, accordingly.

the most relevant terms are sufficient to be included in the potential, so the summation is performed only for the following magnetic vector charges with the shortest length 1 (see figure 2(*a*)):

$$\pm\mathbf{e}_1, \pm\mathbf{e}_2, \text{and } \pm(\mathbf{e}_1 - \mathbf{e}_2). \tag{13}$$

From the formula, equation (B.3), the RG eigenvalue of $\mathcal{L}_2$ is given by $2 - K/2$ on S_0. It thus becomes relevant for $K < 4$ and brings about the disordered phase.

Theoretically, it has been expected that the critical intermediate phase ($T_{\mathrm{L}} \leqslant T \leqslant T_{\mathrm{H}}$) survives for the case $p \geqslant 4$ [20], and also that the point $K = K_{\mathrm{L}}$ ($\equiv p^2/3$) ($K = K_{\mathrm{H}}$ ($\equiv 4$)) where $\mathcal{L}_1$ ($\mathcal{L}_2$) becomes marginal corresponds to T_{L} (T_{H}) [28]. In [28], we observed the existence of the critical intermediate phase for the $p = 6$ case by the use of the numerical method. Further, since the effective field theory possesses the duality nature which is not obvious in the lattice model, we checked the validity of our theory on the self-dual point deep in the intermediate phase, and also estimated $T_{\mathrm{L,H}}$ semiquantitatively. Here, we shall perform the detailed analysis of the system in the vicinity of the two phase transition points.

2.2. Operator product expansions, three-point functions and remarks

To utilize the CFT technology, we shall first clarify the relationship among local operators which plays an important role in our discussion. Since the intermediate region corresponds to the Gaussian fixed line parameterized by K, the so-called $\mathcal{M}$ operator [37, 38],

$$\mathcal{M}(\mathbf{x}) \equiv \frac{Ka^2}{\sqrt{8}} \sum_{i=x,y} \|\partial_i \mathbf{\Phi}(\mathbf{x})\|^2 \tag{14}$$

which is proportional to $\mathcal{L}_0$ and translates the system along the line, is the most important one. The two-point function is given by $\langle \mathcal{M}(\mathbf{x})\mathcal{M}(\mathbf{0})\rangle_0 = (a/r)^4$ so that equation (14) defines the truly marginal operator satisfying the normalization condition. Adding to this, we define the local operators proportional to $\mathcal{L}_{1,2}$ as

$$\mathcal{V}(\mathbf{x}) \equiv \frac{1}{\sqrt{6}} \sum_{\|\mathbf{M}\|=pa^*} :\mathrm{e}^{\mathrm{i}\mathbf{M}\cdot\mathbf{\Phi}(\mathbf{x})}:, \tag{15}$$

$$\mathcal{W}(\mathbf{x}) \equiv \frac{1}{\sqrt{6}} \sum_{\|\mathbf{N}\|=1} :\mathrm{e}^{\mathrm{i}\mathbf{N}\cdot\mathbf{\Theta}(\mathbf{x})}:. \tag{16}$$

Their two-point functions are $\langle \mathcal{V}(\mathbf{x})\mathcal{V}(\mathbf{0})\rangle_0 = (a/r)^{2x_{\mathcal{V}}}$ and $\langle \mathcal{W}(\mathbf{x})\mathcal{W}(\mathbf{0})\rangle_0 = (a/r)^{2x_{\mathcal{W}}}$ with the dimensions

$$x_{\mathcal{V}} \equiv \frac{2p^2}{3K} \qquad \text{and} \qquad x_{\mathcal{W}} \equiv \frac{K}{2}, \tag{17}$$

so they are also in the normalized forms.

First, let us consider the expansion of the operator product $\mathcal{V}(\mathbf{x})\mathcal{V}(\mathbf{0})$, which becomes important for $K \simeq K_{\mathrm{L}}$. While there are 36 terms in the double summations with respect to the vector charges, say, $\mathbf{M}$ and $\mathbf{M}'$, the following two cases are enough to be taken into account: (i) $\mathbf{M} + \mathbf{M}' = \mathbf{0}$ (six terms) and (ii) $\|\mathbf{M} + \mathbf{M}'\| = pa^*$ (12 terms); the other 18 terms are irrelevant. After some calculations using the basic relations in appendices, we find that the cases (i) and (ii) mainly give $\mathcal{M}$ and $\mathcal{V}$, respectively. We then obtain the expression of the OPE as follows:

$$\mathcal{V}(\mathbf{x})\mathcal{V}(\mathbf{0}) \simeq -\frac{x_{\mathcal{V}}}{\sqrt{2}}\left(\frac{a}{r}\right)^{2x_{\mathcal{V}}-2}\mathcal{M}(\mathbf{0}) + \frac{2}{\sqrt{6}}\left(\frac{a}{r}\right)^{x_{\mathcal{V}}}\mathcal{V}(\mathbf{0}) + \cdots. \tag{18}$$

The part '$\cdots$' includes the unit operator, the stress tensor as well as less singular terms. It should be noted that the second term in the right-hand side (rhs) appears due to the triangular-lattice structure of $\mathcal{R}^*$, which is highly contrasted to the single component case, and brings about differences as we will see in the following. The cross-check of equation (18) can be done by performing the another OPE calculation

$$\mathcal{M}(\mathbf{x})\mathcal{V}(\mathbf{0}) \simeq -\frac{x_{\mathcal{V}}}{\sqrt{2}}\left(\frac{a}{r}\right)^2 \mathcal{V}(\mathbf{0}) + \cdots, \tag{19}$$

which exhibits the symmetry property of the OPE coefficients to satisfy, i.e., $C_{\mathcal{V}\mathcal{V}\mathcal{M}} = C_{\mathcal{M}\mathcal{V}\mathcal{V}}$ $(=C_{\mathcal{V}\mathcal{M}\mathcal{V}})$. Now, we can read off the OPE coefficients as follows:

$$C_{\mathcal{V}\mathcal{V}\mathcal{M}} = -\frac{x_{\mathcal{V}}}{\sqrt{2}} \qquad \text{and} \qquad C_{\mathcal{V}\mathcal{V}\mathcal{V}} = \frac{2}{\sqrt{6}}. \tag{20}$$

Next, we shall consider the region near $K \simeq K_{\mathrm{H}}$, and derive the OPE of $\mathcal{W}(\mathbf{x})\mathcal{W}(\mathbf{0})$. Using the basic relations in appendices, it proceeds in parallel with the derivations of equations (18) and (19). Then, we obtain

$$\mathcal{W}(\mathbf{x})\mathcal{W}(\mathbf{0}) \simeq \frac{x_{\mathcal{W}}}{\sqrt{2}}\left(\frac{a}{r}\right)^{2x_{\mathcal{W}}-2} \mathcal{M}(\mathbf{0}) + \frac{2}{\sqrt{6}}\left(\frac{a}{r}\right)^{x_{\mathcal{W}}} \mathcal{W}(\mathbf{0}) + \cdots, \tag{21}$$

$$\mathcal{M}(\mathbf{x})\mathcal{W}(\mathbf{0}) \simeq \frac{x_{\mathcal{W}}}{\sqrt{2}}\left(\frac{a}{r}\right)^2 \mathcal{W}(\mathbf{0}) + \cdots. \tag{22}$$

Thus, the OPE coefficients are given by

$$C_{\mathcal{W}\mathcal{W}\mathcal{M}} = \frac{x_{\mathcal{W}}}{\sqrt{2}} \qquad \text{and} \qquad C_{\mathcal{W}\mathcal{W}\mathcal{W}} = \frac{2}{\sqrt{6}}, \tag{23}$$

where the nonzero $C_{\mathcal{W}\mathcal{W}\mathcal{W}}$ is again attributed to the triangular-lattice structure of the repeat lattice $\mathcal{R}$.

As one of the consequences of the above OPE calculations, we can fix the three-point functions among operators. In contrast to the single component case, we obtain the nonvanishing one for the phase locking potentials, e.g,

$$\langle \mathcal{V}(\mathbf{x}_1)\mathcal{V}(\mathbf{x}_2)\mathcal{V}(\mathbf{x}_3)\rangle_0 = C_{\mathcal{V}\mathcal{V}\mathcal{V}} \prod_{1\leqslant j<k\leqslant 3}\left(\frac{a}{r_{jk}}\right)^{x_{\mathcal{V}}}, \tag{24}$$

where r_{jk} is the distance between $\mathbf{x}_j$ and $\mathbf{x}_k$ (the same relation also holds for $\mathcal{W}$). This is because three vectors at the angle of 120° to each other (e.g., $p\,\mathbf{e}^1$, $p\,\mathbf{e}^2$ and $-p(\mathbf{e}^1+\mathbf{e}^2)$, as visible in figure 2(*b*)) satisfy *the vector charge neutrality condition* [20, 28] (an extension of the scalar case [37, 38]), and this plays an important role in the following discussion.

Lastly, we shall refer to other operators not listed above. The spin degrees of freedom is the most basic one, and is defined as $S_k \equiv :\mathrm{e}^{\mathrm{i}\varphi_k}:$. In the previous paper, based on its response to the spin rotations, equation (3), we argued that its sublattice dependent expression is given by

$$(S_{\mathrm{a}}, S_{\mathrm{b}}, S_{\mathrm{c}}) = \left(:\mathrm{e}^{\mathrm{i}(\mathbf{e}^1+\mathbf{e}^2)\cdot\boldsymbol{\Phi}}:, :\mathrm{e}^{-\mathrm{i}\mathbf{e}^1\cdot\boldsymbol{\Phi}}:, :\mathrm{e}^{-\mathrm{i}\mathbf{e}^2\cdot\boldsymbol{\Phi}}:\right), \tag{25}$$

whose dimensions are all $x_S = 2/3K$ (see equation (B.3)) [28]. This is one example of a general form of the quantities related to the spin degrees of freedom, i.e.,

$$\mathcal{O}(\mathbf{x}; \{w_{\mathbf{M}}\}) \equiv \sum_{\|\mathbf{M}\|=M} w_{\mathbf{M}} : \mathrm{e}^{\mathrm{i}\mathbf{M}\cdot\boldsymbol{\Phi}} : (w_{\mathbf{M}} \in \mathbb{C}). \tag{26}$$

For instance, for $S_{\mathrm{a}}(\mathbf{x})$, the length of vector charges M equals to a^*, and the weights are given by $(w_{\mathbf{e}^1}, w_{\mathbf{e}^1+\mathbf{e}^2}, w_{\mathbf{e}^2}, w_{-\mathbf{e}^1}, w_{-\mathbf{e}^1-\mathbf{e}^2}, w_{-\mathbf{e}^2}) = (0, 1, 0, 0, 0, 0)$. In the above,

we observed that *the uniform mode* whose weights are independent of the direction of **M** is engaged in the Lagrangian density due to its symmetry property (see the definition of $\mathcal{V}$ in equation (15)). However, it is also expected that *the staggered mode* with $(w_{p\mathbf{e}^1}, w_{p(\mathbf{e}^1+\mathbf{e}^2)}, w_{p\mathbf{e}^2}, w_{-p\mathbf{e}^1}, w_{-p(\mathbf{e}^1+\mathbf{e}^2)}, w_{-p\mathbf{e}^2}) = (+1, -1, +1, -1, +1, -1)$ plays an important role, while we shall not discuss this issue in detail.

2.3. Renormalization-group equations

Since the data necessary for the use of the CFT technology have been obtained, we shall here perform the RG analysis of our effective field theory. First, we consider the region near $K \simeq K_{\mathrm{L}}$, where $\mathcal{L}_2$ is irrelevant. For convenience, we define the scaling field y_0 as

$$K = (1 + y_0)K_{\mathrm{L}}. \tag{27}$$

Then, the system can be described by the fixed-point Lagrangian density (or CFT) $\mathcal{L}_0^{\mathrm{L}}$ (i.e., the Gaussian part with K_{L}) perturbed by two marginal operators $\mathcal{M}$ and $\mathcal{V}$ as

$$\mathcal{L} \simeq \mathcal{L}_0 + \mathcal{L}_1 = \mathcal{L}_0^{\mathrm{L}} + \frac{\sqrt{2}y_0}{2\pi a^2}\mathcal{M}(\mathbf{x}) + \frac{\sqrt{6}y_p}{2\pi a^2}\mathcal{V}(\mathbf{x}). \tag{28}$$

For a perturbed CFT defined by the Lagrangian density, $\mathcal{L}_{\mathrm{gen.}} = \mathcal{L}_0^* + \sum_\mu \lambda_\mu \mathcal{O}_\mu(\mathbf{x})/2\pi a^2$, where marginal scalar operators $\mathcal{O}_\mu$ are normalized as $\langle \mathcal{O}_\mu(\mathbf{x})\mathcal{O}_\nu(\mathbf{0})\rangle_0^* = \delta_{\mu\nu}\,(a/r)^4$ ($\langle\cdots\rangle_0^*$ means the average at the fixed point under consideration), the one-loop RG equations are governed by the OPE coefficients: for the change, $a \to (1 + \mathrm{d}l)a$, they are given by $\mathrm{d}\lambda_\mu/\mathrm{d}l = -\frac{1}{2}\sum_{\nu,\rho} C^*_{\mu\nu\rho}\lambda_\nu\lambda_\rho$ ($C^*_{\mu\nu\rho}$ denotes the value on $\mathcal{L}_0^*$) [39]. In the present case, using coefficients of equation (20) at $K = K_{\mathrm{L}}$, we obtain the following equations:

$$\frac{\mathrm{d}y_0(l)}{\mathrm{d}l} = 3y_p(l)^2, \tag{29}$$

$$\frac{\mathrm{d}y_p(l)}{\mathrm{d}l} = 2y_0(l)y_p(l) - y_p(l)^2. \tag{30}$$

Similarly to the BKT RG-flow diagram, these exhibit one separatrix between the ordered and the critical phases, i.e.,

$$y_p(l) = -y_0(l), \tag{31}$$

and one straight flow, $y_p(l) = 2y_0(l)/3$, renormalized to the strong-coupling fixed point (see the right panel in figure 3). These are similar to those obtained in the research on the triangular-lattice defect melting problem [26, 40] (see also [20]). Consequently, we can introduce the small parameter t to control the distance from the separatrix as

$$y_p(l) = -(1 + t)y_0(l)\ (|t| \ll 1). \tag{32}$$

Next, we shall derive the RG equations near $K \simeq K_{\mathrm{H}}$, where $\mathcal{L}_1$ is irrelevant. We redefine the scaling field y_0 as

$$K = (1 + y_0)K_{\mathrm{H}}. \tag{33}$$

Then, the system is described by

$$\mathcal{L} \simeq \mathcal{L}_0 + \mathcal{L}_2 = \mathcal{L}_0^{\mathrm{H}} + \frac{\sqrt{2}y_0}{2\pi a^2}\mathcal{M}(\mathbf{x}) + \frac{\sqrt{6}y_1}{2\pi a^2}\mathcal{W}(\mathbf{x}), \tag{34}$$

where $\mathcal{L}_0^{\mathrm{H}}$ is the fixed-point Lagrangian density for the high-temperature transition. The RG equations are similarly obtained as follows:

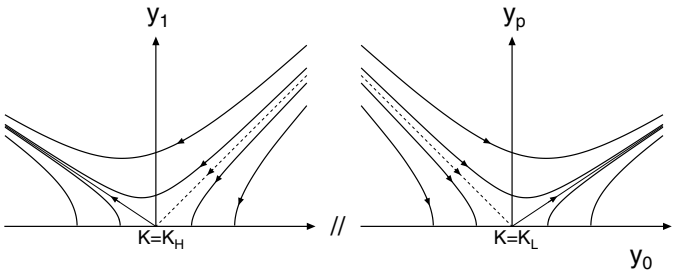

Figure 3. The schematic RG-flow diagram. The left (right) panel exhibits the flow around the multicritical fixed point $(y_0, y_1) = (0, 0)$ $[(y_0, y_p) = (0, 0)]$ corresponding to the transition temperature $T_{\rm H}(T_{\rm L})$. The scale of y_0 in the left is different from that in the right, and y_1 and y_p axes are not on the same plain. The separatrixes around the points are given by the dotted lines.

$$\frac{{\rm d}y_0(l)}{{\rm d}l} = -3y_1(l)^2, \tag{35}$$

$$\frac{{\rm d}y_1(l)}{{\rm d}l} = -2y_0(l)y_1(l) - y_1(l)^2. \tag{36}$$

Since these are related to equations (29) and (30) via the replacement $(y_0, y_p) \to (-y_0, y_1)$, one separatrix between the disordered and the critical phases,

$$y_1(l) = y_0(l), \tag{37}$$

and one straight flow, $y_1(l) = -2y_0(l)/3$, renormalized to the high-temperature fixed point, are embedded (see the left panel in figure 3). Thus, for the same aim, we shall introduce the small parameter t as

$$y_1(l) = (1 + t)y_0(l) \ (|t| \ll 1). \tag{38}$$

Here, we note that Boyanovsky and Holman performed the RG of the vectorial sine-Gordon field theory based on the simply-laced Lie algebras [41]. While they provided a general argument on properties of operators, and some of them are the same as those observed above, we have focused on $\mathcal{L}$ corresponding to the specific model, TSIM.

2.4. Mixing of marginal operators

According to one of the present authors' discussion for the sine-Gordon field theory, linear combinations of marginal operators play an important role [29]. As we see in the following, it is true also in the present case. So, we shall consider this issue in this subsection. Let us start with the system around the separatrix equation (31), and consider the following quantities:

$$\mathcal{A} \propto \mathcal{M} + c_1\mathcal{V} \qquad \text{and} \qquad \mathcal{B} \propto \mathcal{V} + c_2\mathcal{M}. \tag{39}$$

The two real coefficients $c_{1,2}$ are to be determined from the orthogonality condition $\langle \mathcal{A}(\mathbf{x}_1)\mathcal{B}(\mathbf{x}_2)\rangle = 0$ which persists under the renormalization along the separatrix (while the normalization conditions, e.g., $\langle \mathcal{A}(\mathbf{x}_1)\mathcal{A}(\mathbf{x}_2)\rangle = (a/r_{12})^4$, are used to determine overall constants). Instead of the correlation function, we consider a more convenient quantity [42]

$$F(r_{12}, a, y_0(l), y_p(l)) \equiv \left(\frac{r_{12}}{a}\right)^4 \langle \mathcal{A}(\mathbf{x}_1)\mathcal{B}(\mathbf{x}_2)\rangle, \tag{40}$$

and evaluate F and its response to the change of the cutoff $\mathrm{d}F/\mathrm{d}l$ up to the lowest order in the coupling constants y_0 and y_p. For this, we first expand F with respect to y_p as

$$F(r_{12}, a, y_0, y_p) \simeq F_0(r_{12}, a, y_0) - \sqrt{6} y_p F_1(r_{12}, a, y_0), \tag{41}$$

where

$$F_0 = \left(\frac{r_{12}}{a}\right)^4 \langle \mathcal{A}(\mathbf{x}_1)\mathcal{B}(\mathbf{x}_2)\rangle_0, \tag{42}$$

$$F_1 = \left(\frac{r_{12}}{a}\right)^4 \int \frac{\mathrm{d}^2 x_3}{2\pi a^2} \langle \mathcal{A}(\mathbf{x}_1)\mathcal{B}(\mathbf{x}_2)\mathcal{V}(\mathbf{x}_3)\rangle_0. \tag{43}$$

We should regularize the UV divergence of the integral over $\mathbf{x}_3$ in equation (43) by excluding two circles of the radius a centered at $\mathbf{x}_1$ and $\mathbf{x}_2$. Explicitly, the integral is restricted as

$$\int \to \int H(r_{13} - a) H(r_{23} - a), \tag{44}$$

where $H(x)$ is the Heaviside step function. Noting $4 - 2x_{\mathcal{V}} \simeq 4y_0$, we can rewrite equation (42) as $F_0 \simeq c_1 + c_2 + 4c_1 y_0 \ln(r_{12}/a)$. This exhibits F being almost constant $F \simeq c_1 + c_2$, so the condition in the lowest order,

$$c_1 + c_2 = 0, \tag{45}$$

should be satisfied. Next, let us consider its response to the change of the cutoff, $\mathrm{d}F_0/\mathrm{d}l$. There exist two types of contributions, i.e., (i) a direct one via the cutoff a and (ii) an indirect one via the coupling constant y_0 controlled by the RG equations. Since the β-functions equations (29) and (30) only include the second-order terms, we can neglect the latter. Then, we obtain

$$\frac{\mathrm{d}F_0}{\mathrm{d}l} \simeq -4c_1 y_0. \tag{46}$$

The contributions from the change of the coupling constant y_p to the response of the second term in equation (41) can be neglected due to the same reason, so we shall consider $\mathrm{d}F_1/\mathrm{d}l$ up to the zeroth order in y_0. Like the case of the first term, there also exist two types of contributions; we can omit the type (ii) contributions. Furthermore, as we have already seen in the derivation of equation (46), a part of the type (i) contributions stemming from the power-of-a factors and giving the $\mathrm{O}(y_0)$ terms can be neglected. Consequently, the response is contributed only from the change of a in the UV regularization factor

$$\frac{\mathrm{d}F_1}{\mathrm{d}l} \simeq \left(\frac{r_{12}}{a}\right)^4 \int \frac{\mathrm{d}^2 x_3}{2\pi a^2} \langle \mathcal{A}(\mathbf{x}_1)\mathcal{B}(\mathbf{x}_2)\mathcal{V}(\mathbf{x}_3)\rangle_0^{\mathrm{L}} \frac{\mathrm{d}}{\mathrm{d}l}[H(r_{31} - a)H(r_{32} - a)]. \tag{47}$$

Since the integral is a line one along two circumferences of circles centered at $\mathbf{x}_1$ and $\mathbf{x}_2$, we can estimate the rhs of equation (47) by using the asymptotic form of the three-point functions (e.g., equation (24)); the result is the following:

$$\frac{\mathrm{d}F_1}{\mathrm{d}l} \simeq -2\left[C^{\mathrm{L}}_{\mathcal{M}\mathcal{V}\mathcal{V}}(1 + c_1 c_2) + C_{\mathcal{V}\mathcal{V}\mathcal{V}} c_1\right], \tag{48}$$

where $C^{\mathrm{L}}_{\mathcal{M}\mathcal{V}\mathcal{V}} = -\sqrt{2}$. Consequently, from the lowest-order calculation of the condition $\mathrm{d}F/\mathrm{d}l = 0$, we obtain the relation $c_1 y_0 + [\sqrt{3}(1 + c_1 c_2) - c_1] y_p = 0$. On the separatrix $y_p = -y_0$, this is reduced to

$$2c_1 - \sqrt{3}(1 + c_1 c_2) = 0, \tag{49}$$

which, together with equation (45), can determine the coefficients. While the quadratic equation for c_1, $c_1^2 + 2c_1/\sqrt{3} - 1 = 0$, possesses two solutions $1/\sqrt{3}$ and $-\sqrt{3}$, both of these provide an identical description of the operators. Thus, in the following discussion, we choose $c_1 = 1/\sqrt{3}$, and call $\mathcal{A}$ and $\mathcal{B}$ as the $\mathcal{M}$-like and the $\mathcal{V}$-like operators, respectively (see reference [29]). Their normalized expressions are then given by

$$\begin{pmatrix} \mathcal{A} \\ \mathcal{B} \end{pmatrix} = \begin{pmatrix} \cos\vartheta_{\mathrm{L}} & \sin\vartheta_{\mathrm{L}} \\ -\sin\vartheta_{\mathrm{L}} & \cos\vartheta_{\mathrm{L}} \end{pmatrix} \begin{pmatrix} \mathcal{M} \\ \mathcal{V} \end{pmatrix} \tag{50}$$

with $\tan\vartheta_{\mathrm{L}} = 1/\sqrt{3}$. Here, note the followings: since the condition to determine the mixing angle ϑ_{L}, equation (49), is expressed in terms of the OPE coefficients, we can recognize it as an appearance of the universal properties of the fixed point $\mathcal{L}_0^{\mathrm{L}}$. Further, in the single component case, the corresponding mixing angle is given by $\tan\vartheta = 1/\sqrt{2}$ [29]. This difference mainly stems from the $C_{\mathcal{V}\mathcal{V}\mathcal{V}}$ contribution absent in the scalar case.

Next, let us move on to the region near T_{H}, and consider the system around the separatrix equation (37), where the following linear combinations are to be determined:

$$\mathcal{C} \propto \mathcal{M} + d_1\mathcal{W} \qquad \text{and} \qquad \mathcal{D} \propto \mathcal{W} + d_2\mathcal{M}. \tag{51}$$

In the same way as the above, the orthogonality condition $\langle \mathcal{C}(\mathbf{x}_1)\mathcal{D}(\mathbf{x}_2)\rangle = 0$ persisting under the renormalization along the separatrix determines the real coefficients $d_{1,2}$. Since the calculations are performed in parallel with the above case, we can straightforwardly derive the equations corresponding to equations (45) and (49) as $d_1 + d_2 = 0$ and $2d_1 + \sqrt{3}(1 + d_1 d_2) = 0$, respectively. In accordance with the above case, the solution $d_1 = -1/\sqrt{3}$ is chosen, so that $\mathcal{C}$ and $\mathcal{D}$ are termed as the $\mathcal{M}$-like and the $\mathcal{W}$-like operators, respectively (the difference between $\mathcal{A}$ and $\mathcal{C}$ is contextually obvious). The normalized expressions are then given as follows:

$$\begin{pmatrix} \mathcal{C} \\ \mathcal{D} \end{pmatrix} = \begin{pmatrix} \cos\vartheta_{\mathrm{H}} & \sin\vartheta_{\mathrm{H}} \\ -\sin\vartheta_{\mathrm{H}} & \cos\vartheta_{\mathrm{H}} \end{pmatrix} \begin{pmatrix} \mathcal{M} \\ \mathcal{W} \end{pmatrix} \tag{52}$$

with $\tan\vartheta_{\mathrm{H}} = -1/\sqrt{3}$. Consequently, independently of p, we find a simple relation between the mixing angles at the high- and the low-temperature transitions, $\vartheta_{\mathrm{L}} = -\vartheta_{\mathrm{H}}$ $(= \pi/6)$.

2.5. Corrections to finite-size scaling and eigenvalue structures

We are in a position to calculate the renormalized scaling dimensions of operators around the fixed points $\mathcal{L}_0^{\mathrm{L,H}}$ and to discuss the significance of the results above. We shall start from the free part defined on an infinitely long cylinder in the x_2-direction with a periodicity of L in the x_1-direction, and write the partition function using the action $S_{0,\mathrm{cyl.}} \equiv \int_{\mathrm{cyl.}} \mathrm{d}^2x\mathcal{L}_0$ as $Z_{0,\mathrm{cyl.}} \equiv \int[\mathrm{d}\mathbf{\Phi}]\,\mathrm{e}^{-S_{0,\mathrm{cyl.}}} \propto \lim_{\tau\to\infty}\mathrm{Tr}\,\mathrm{e}^{-\tau\hat{H}_{0,L}}$. Then, $\hat{H}_{0,L}$ exhibits the Hamiltonian operator associated with the transfer matrix $\mathrm{e}^{-\hat{H}_{0,L}}$; it defines a 1D quantum system with length L, and is given by $\hat{H}_{0,L} = \int_0^L \mathrm{d}x_1\hat{\mathcal{H}}_0(x_1)$ with

$$\hat{\mathcal{H}}_0(x) = \frac{v}{2}\left[\frac{\pi}{K}\hat{\pi}_\alpha(x)\hat{\pi}^\alpha(x) + \frac{K}{\pi}\partial_x\hat{\phi}_\alpha(x)\partial_x\hat{\phi}^\alpha(x)\right]. \tag{53}$$

The momentum $\hat{\pi}_\alpha$ conjugate to the field operator $\hat{\phi}^\alpha$ satisfies $[\hat{\phi}^\alpha(x), \hat{\pi}_\beta(x')] = \mathrm{i}\delta^\alpha_\beta\delta(x - x')$, and v is the velocity of an elementary excitation. When we writing its eigenvalue and eigenstate as $E_{0,L,\nu}$ and $|\nu\rangle$, the CFT provides the finite-size-scaling form of the excitation gap as $\Delta E_{0,L,\nu} \equiv E_{0,L,\nu} - E_{0,L,\mathrm{g}} = 2\pi v x_\nu/L$, where $E_{0,L,\mathrm{g}}$ and x_ν are the lowest energy and the scaling dimension of the operator corresponding to the state $|\nu\rangle$ (L is supposed to be large enough). Next, we consider the Hamiltonian density corresponding to the generic

model $\mathcal{L}_{\text{gen.}}$, i.e., $\hat{\mathcal{H}}_{\text{gen.}}(x) = \hat{\mathcal{H}}_0^*(x) + \sum_\mu \lambda_\mu \hat{\mathcal{O}}_\mu(x)/2\pi a^2$. Writing the ground-state and the excited-state energies as $E_{L,\text{g}}$ and $E_{L,\nu}$, then we can calculate the corrections to scaling within the first-order perturbation as $\Delta E_{L,\nu} \equiv E_{L,\nu} - E_{L,\text{g}} \simeq \frac{2\pi v}{L}\left(x_\nu + \sum_\mu \lambda_\mu C^*_{\mu\nu\nu}\right)$ [43]. The parenthesized quantity in the rhs defines the renormalized scaling dimension. Using the OPE coefficients, the mixing angle ϑ_{L}, and this formula, we obtain the dimensions of the $\mathcal{M}$-like and the $\mathcal{V}$-like operators near T_{L} (i.e., near the separatrix equation (32)) as

$$x_{\mathcal{A}} = 2 + 2y_0\left(1 + \frac{5}{4}t\right), \tag{54}$$

$$x_{\mathcal{B}} = 2 - 6y_0\left(1 + \frac{3}{4}t\right). \tag{55}$$

Similarly, we obtain those of the $\mathcal{M}$-like and the $\mathcal{W}$-like operators near T_{H} (equation (38)) as

$$x_{\mathcal{C}} = 2 - 2y_0\left(1 + \frac{5}{4}t\right), \tag{56}$$

$$x_{\mathcal{D}} = 2 + 6y_0\left(1 + \frac{3}{4}t\right) \tag{57}$$

(y_0 was redefined as mentioned above). Since these corrections to scaling are described by the OPE coefficients, there are some universal relations among the dimensions. For instance, in the present case, we find that

$$\frac{3x_{\mathcal{A}} + x_{\mathcal{B}}}{4} = 2 \qquad \text{on} \quad y_p = -y_0, \tag{58}$$

$$\frac{3x_{\mathcal{C}} + x_{\mathcal{D}}}{4} = 2 \qquad \text{on} \quad y_1 = y_0. \tag{59}$$

Since the ratio of the level splitting, 1:3, being different from that in the single component case [29] is one of features, this can provide a solid evidence of the BKT-like phase transition described by the RG equations (29), (30) or equations (35) and (36).

3. Numerical calculations (the $p = 6$ case)

In this section, we shall explain our numerical calculations and results to confirm the above theoretical predictions. We consider the system on Λ with M ($\to\infty$) rows of L (a multiple of 3) sites wrapped on the cylinder, and define the transfer matrix connecting the next-nearest-neighbor rows (see figure 1). We denote its eigenvalues as $\lambda_q(L)$ or their logarithms as $E_q(L) = -\frac{1}{2}\ln|\lambda_q(L)|$ (q specifies a level). Then, the conformal invariance in critical systems provides the expressions of the central charge c and the scaling dimension x_q as the corrections to scaling [44–46]

$$E_{\text{g}}(L) \simeq Lf - \frac{\pi}{6L\zeta}c \qquad \text{and} \qquad \Delta E_q(L) \simeq \frac{2\pi}{L\zeta}x_q. \tag{60}$$

Here, $E_{\text{g}}(L)$, $\Delta E_q(L)$ ($=E_q(L) - E_{\text{g}}(L)$), ζ ($=2/\sqrt{3}$), and f correspond to 'the ground-state energy', 'the excitation gap', the geometric factor and a free energy density, respectively. In numerical diagonalization calculations using the Lanczos algorithm, we employ two fundamental spin rotations $\hat{R}_{\text{a}}$ and $\hat{R}_{\text{b}}$ in equation (3) as well as the lattice translation and the space inversion. This is because the matrix size can be reduced, and more importantly

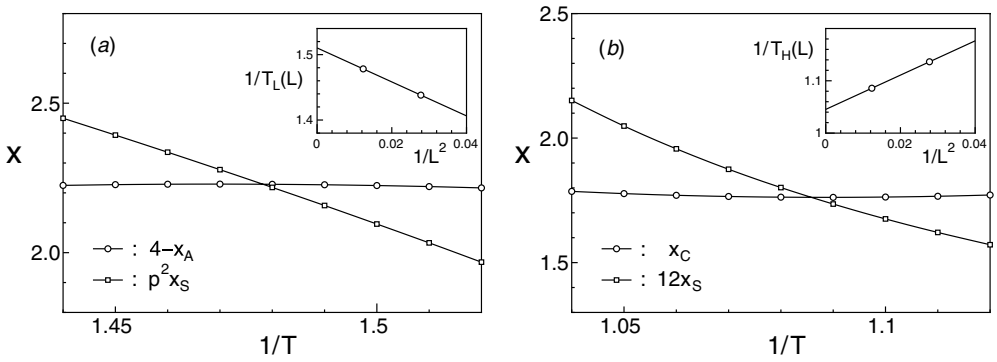

Figure 4. (*a*) The plot of the level-crossing condition of equation (61) (the $p = 6$ case). The circles (squares) with the fitting curve exhibit its rhs (lhs). The crossing point gives the finite-size estimate of the phase transition point $1/T_{\rm L}(L)$ with $L = 9$. The inset shows the extrapolation of the data to the thermodynamic limit, and gives $1/T_{\rm L} \simeq 1.51$. (*b*) The same plot of equation (62) as the panel (*a*), where the circles (squares) with the fitting curve exhibit the rhs (lhs). The crossing point estimates $1/T_{\rm H}(L)$ with $L = 9$. The inset shows the extrapolation of the finite system data, and gives $1/T_{\rm H} \simeq 1.05$.

discrete symmetries can specify lower-energy excitations. For instance, since the spin degrees of freedom on $\Lambda_{\rm a}$ transforms as $\hat{R}_{\rm a} S_k \mapsto {\rm e}^{{\rm i}2\pi/p} S_k$ and $\hat{R}_{\rm b} S_k \mapsto S_k$, the corresponding excitation level can be found in the sector with indexes $({\rm e}^{{\rm i}2\pi/p},1)$, and provides a small scaling dimension $x_S = 2/3K$ [28]. Thus, we shall utilize also this level for the determinations of the phase transition points.

First, we consider the system around the separatrix equation (31). From equation (54) and the dimension of the sublattice dependent spin, $x_S \simeq 2(1 - y_0)/p^2$, the condition

$$p^2 x_S = 4 - x_{\mathcal{A}} \tag{61}$$

is satisfied at $t = 0$ (i.e., on the separatrix equation (31)). Thus, it can be employed as a criterion to determine the low-temperature transition point $T_{\rm L}$. We perform the numerical calculations for the $p = 6$ case and for the systems up to $L = 9$. In figure 4(*a*), we exhibit temperature dependences of the scaling dimensions, i.e., the both sides of equation (61) estimated for the $L = 9$ site system, and find the level crossing at which the condition is satisfied. Therefore, we obtain the finite-size estimate, $1/T_{\rm L}(L)$, from the crossing point. As we show in the inset, the extrapolation of finite-size estimates to the thermodynamic limit is performed based on the least-squares-fitting procedure $1/T_{\rm L}(L) = 1/T_{\rm L} + a/L^2$. Then, we obtain the transition point as $1/T_{\rm L} \simeq 1.51$.

Second, we consider the determination of $T_{\rm H}$, which can be performed in the parallel way to the above. From equation (56) and the dimension of spin, $x_S \simeq (1 - y_0)/6$, around equation (37), the condition

$$12 x_S = x_{\mathcal{C}} \tag{62}$$

is found to be satisfied only on the separatrix. In figure 4(*b*), we provide the same plot as figure 4(*a*), where the circles (squares) with the fitting curve plot the rhs (lhs) of equation (62). Again, we find the level crossing at which the condition is satisfied. Therefore, we can estimate $1/T_{\rm H}(L)$ from the crossing point. The extrapolation to the limit $L \to \infty$ is also performed (see the inset), and then we estimate the high-temperature transition point as $1/T_{\rm H} \simeq 1.05$.

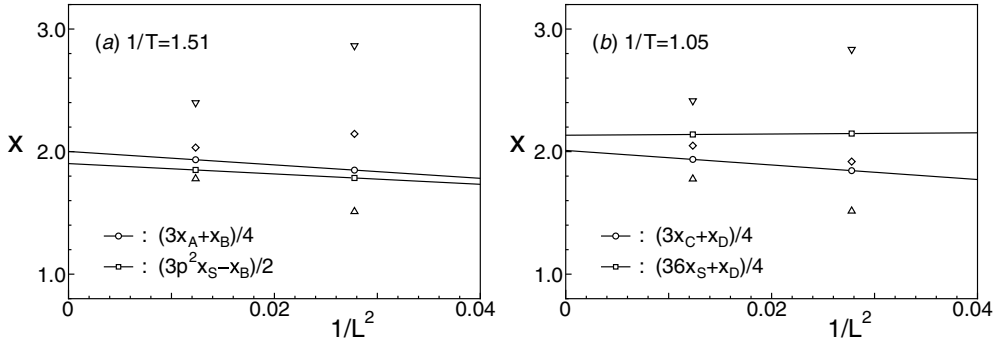

Figure 5. (*a*) The check of the universal relations among scaling dimensions at T_{L}. The circles (squares) with the fitting line plot the lhs of equation (58) (the difference $(3p^2x_S - x_B)/2$) at $1/T = 1.51$. The up- and the down-ward triangles show x_A and x_B, respectively, and the diamonds plot p^2x_S (with $p = 6$). (*b*) The check of the universal relations at T_{H}. The circles (squares) with the fitting line plot the lhs of equation (59) (the average $(36x_S + x_D)/4$) at $1/T = 1.05$. The up- and the down-ward triangles show x_C and x_D, respectively, and the diamonds plot $36x_S$.

In the previous paper, we roughly estimated the transition points from the behavior of the central charge (i.e., deviations from the theoretical value $c = 2$), and obtained $1/T_{\mathrm{L,H}} \simeq 1.5$, 1.1, respectively. Thus, our above estimates through the level crossings are found to be consistent with the data of the central charge.

At this stage, it is important to check the universal relations among the scaling dimensions. As mentioned, since the relation, equation (58), must hold between the $\mathcal{M}$-like and the $\mathcal{V}$-like excitations at T_{L}, we calculate the average (i.e., its lhs) at $1/T = 1.51$. As is shown in figure 5(*a*), the estimates converge to the theoretical value 2 very accurately (see the circles with fitting line), meanwhile the scaling dimensions themselves considerably deviate from 2 (see the up- and the down-ward triangles). Further, the relation $(3p^2x_S - x_B)/2 = 2$ is also expected to hold at the transition point, so we calculate the difference (the $p = 6$ case), and plot the data in the same figure (see the square with the fitting line). Despite the smallness of the system sizes, the relation holds within 5% error. These checks can be passed only if the system is at the BKT-like phase transition point, and the numerically utilized levels possess the theoretically expected properties. Therefore, these are helpful to demonstrate the reliability of our approach and results.

We perform the same checks for the high-temperature transition. In figure 5(*b*), we plot the average (the lhs of equation (59)) at $1/T = 1.05$. We find the excellent convergence of the data to 2 in the thermodynamic limit (see the circles with fitting line). In addition, another relation $(36x_S + x_D)/4 = 2$ is expected between the dimensions of the spin and the $\mathcal{W}$-like operators; we plot the average in the same figure (see the square with fitting line). Then, we find the deviation of the limiting value ($\simeq$2.13) from 2. This may be due to the following reason: in the thermodynamic limit, the universal jump of $K(l = \infty)$ from K_{H} (=4) to 0 occurs at T_{H}, and x_S is inversely depending upon K (see equation (B.3)). Therefore, x_S is sensitive to the temperature. T_{H} was reliably estimated from the level crossing, but due to the limitation in the size of systems treated, it may include some error which causes the deviation.

Consequently, we have applied the level-crossing conditions to determine the BKT-like transition points, and then we have checked some universal relations among excitation levels at the transition points. This strategy (the level spectroscopy) was proposed and developed by one of the present authors to analyze the BKT transitions in 1D quantum spin systems [29].

In that case, the sine-Gordon field theory is relevant to the discussion. On the other hand, since the present BKT-like transitions are described by the vector sine-Gordon models, we have extended the strategy to be applicable to them. Then, we have successfully demonstrated its efficiency through the numerical calculations of TSIM.

4. Discussion and summary

Up to now, we have concentrated on the properties of the critical intermediate phase: it possesses the conformal symmetry with $c = 2$, and exhibits the transitions to the ordered and the disordered phases. While, for the latter, its similarity to the triangular-lattice defect melting phenomena was argued in the literature [20, 28], we shall re-visit the universality class of the transition, and refer to its relevance to a ground-state phase transition observed in a quantum spin chain system.

In the limit $p \to \infty$, the symmetry of TSIM ($\mathbb{Z}_p \times \mathbb{Z}_p$) becomes the U(1) $\times$ U(1), i.e., the continuous one, and eliminates the low-temperature ordered phase. The RG-flow equations (35) and (36) still describe the transition to the disordered phase, and enable us to analyze the system around the transition point. Based on them, quite recently, one of the authors proposed a finite-size-scaling ansatz for the helicity modulus of TSIM [47], which has a great relevance to the transition (see also [48–50]). The ansatz reflects a self-similarity of trajectories with respect to a conserved quantity of the flow, and mainly predicts the following: (i) in the disordered phase, the correlation length is given by $\xi \propto \exp[\text{const}/(T - T_{\text{H}})^{\bar{\nu}}]$ with the exponent $\bar{\nu} = 3/5$. (ii) The finite-size-scaling function takes a universal value at the transition temperature, which comes from the RG flow along the separatrix $y_1 = y_0$. While we performed large-scale Monte Carlo (MC) simulations of TSIM in this limit to verify the predictions, here we only mention that simulation data exhibit a good agreement with the ansatz (the readers interested in the detailed discussions and the calculation results may refer to reference [47]). Since it includes the prediction also in the disordered phase, its confirmation is complementary to the present argument of section 2 and 3, and thus provides another solid evidence to support our theoretical description. Simultaneously, the exponent $\bar{\nu} = 3/5$ does not agree with the previous research [20], where $\bar{\nu} = 2/5$ was predicted based on the vector CG representation and the RG argument on the triangular-lattice defect melting theory [25]. Also, in the previous paper [28], the explanation that $\bar{\nu}$ takes $2/5$ was given based on their arguments. But, now we are confident that the exponent should be $3/5$, so the reason of this discrepancy should be clarified in future.

Instead of in the 2D classical systems, we can find the same situation in the ground state of a 1D quantum system. TSIM is invariant under the symmetry group S_3 of the sublattice permutations, and exhibits the conformal invariance with $c = 2$ which stems from the continuous symmetry in the $p \to \infty$ limit. Guided by these properties, we are led to think of the quantum lattice gas model with three components because it realizes the S_3 symmetry as permutations of components, and its exact solution shows the $c = 2$ criticality [51–53]. Also, as its extension, the bilinear-biquadratic (BLBQ) spin-1 chain is widely known, and is defined by the Hamiltonian:

$$H_{\text{BLBQ}} = \sum_{\langle j,k \rangle} [\cos\theta \mathbf{S}_j \cdot \mathbf{S}_k + \sin\theta (\mathbf{S}_j \cdot \mathbf{S}_k)^2]. \tag{63}$$

This model possesses some points where the exact information is available: The Affleck–Kennedy–Lieb–Tasaki point [54], the Takhatajan–Babujian (TB) point ($\theta_{\text{BT}} = -\pi/4$) [55, 56], and the Uimin–Lai–Sutherland (ULS) point ($\theta_{\text{ULS}} = \pi/4$) [51–53]. The last one which corresponds to the quantum lattice gas model separates the extended critical phase

($\pi/2 \geqslant \theta \geqslant \theta_{\rm ULS}$) [57, 58] and the Haldane phase ($\theta_{\rm ULS} > \theta > \theta_{\rm TB}$) [59], and it is described by the level-1 SU(3) Wess–Zumino–Witten model. The central charge for the former and the correlation length in the latter were calculated as $c = 2$ and $\xi \propto \exp[\text{const}/(\theta_{\rm ULS} - \theta)^{3/5}]$, respectively [60], with which the numerical estimations agree [57, 58]. According to the analysis by Itoi and Kato, the critical fixed line does not exist around the ULS point, so the global RG-flow diagram is considerably different from the present one [61]. However, the transition occurs when the system crosses the separatrix with the SU(3) symmetry, and if we focus on the massive region including the transition point, the RG feature is seemingly similar to our case. This may be a reason why the exponent $\bar{\nu}$ takes the same value in both cases. Furthermore, quite recently, the SU(N) self-dual sine-Gordon model consisting of the $(N-1)$-component vectorial fields has been investigated [62, 63]; its relevances to, for instance, the quantum-spin chains (including the BLBQ model) and ladders have been indeed clarified [62]. For TSIM, we have seen that $\mathcal{L}_0$ consists of the two current operators $j^{\alpha}(z)(\alpha = 1, 2)$. In addition, for instance for $K = K_{\rm H}$, the potential $\mathcal{L}_2$ becomes marginal, and the vector charges equation (13) in $\mathcal{R}$ which is isomorphic to the root lattice of the SU(3) Lie algebra provide the six operators $v_{\mathbf{K}}(z)$ with the conformal weight $(\Delta, \overline{\Delta}) = (1, 0)$ (see appendix B). Thus, there exist eight chiral current operators, and they may define the level-1 SU(3) current algebra [64, 65], as in the case of the Kagomé-lattice three-state Potts antiferromagnet [13, 14]. From these all, we think that although TSIM is in the lower symmetry than that of the BLBQ model, it exhibits a symmetry enhancement at the end points of the intermediate phase, and then it may share the same fixed-point properties with the ULS model while more concrete evidences are desired.

Lastly, we shall comment on the $p = 4$ case. Although our theory in section 2 as well as the vector CG analysis [20] predicts the intermediate phase for $4 \leqslant K \leqslant 16/3$, the previous MC data indicated a sign of the first-order transition between the ordered and the disordered phases [19]. However, subsequent studies in computational physics revealed that it is in general difficult to distinguish between the weak first-order and the second-order transitions just based on MC data [66, 67]. Further, there are considerable difficulties also in the treatment of the BKT-like phase transitions (e.g., an accurate determination of the transition point) by MC methods. Thus, for the $p = 4$ case, the nature of phase transitions does not seem to be established yet.

As one of the possibilities, other than equations (4), (5) and (6), there may exist a term inferred from the symmetry consideration, and it might eliminate the intermediate phase as speculated before (see figure 7(*b*) in [20]). Nevertheless, we think that this issue remains as an important future problem.

To summarize, we have investigated the BKT-like continuous phase transitions observed in the triangular-lattice three-spin interaction model (TSIM) based on the vector dual sine-Gordon field theory. The basic properties of the local density operators (e.g., the scaling dimensions) and their mutual relations (the OPE coefficients) have been investigated in detail. Using these CFT data, we have performed the RG analysis of phase transitions and the conformal perturbation calculations of the excitation spectra up to the one-loop order. Especially, the mixing angles of the marginal operators on the separatrixes for the low-temperature and the high-temperature transitions, i.e., $\vartheta_{\rm L,H}$, have been determined and compared to the single component case. Then, we have found some universal relations among the renormalized scaling dimensions, which can precisely characterize the present phase transitions. Furthermore, we have pointed out their importance for the numerical determinations of the phase transition points. To check the theory, we performed the numerical diagonalization calculations of the transfer matrix of TSIM (the $p = 6$ case) up to the system size $L = 9$, and determined the transition points as $1/T_{\rm L,H} = 1.51, 1.05$, respectively, which

was followed by the check of the universal relations among the excitation levels. Lastly, we have discussed the enhancement of symmetry at the end points of the critical intermediate phase. Based on the existence of the eight current operators and the value of the exponent $\bar{\nu} = 3/5$, we have argued its relevance to the ground state of the bilinear-biquadratic spin-1 chain.

Acknowledgments

We thank S Hayakawa, M Iihosi, H Matsuo and M Fujimoto for stimulating discussions. We would like to also thank P Lecheminant for drawing our attention to the [41, 62, 63]. Main computations were performed using the facilities of Information Synergy Center in Tohoku University, Cybermedia Center in Osaka University, and Yukawa Institute for Theoretical Physics in Kyoto University. This work was supported by Grants-in-Aid from the Japan Society for the Promotion of Science, Scientific Research (C), No 17540360 and No 18540376.

Appendix A. Two-dimensional massless scalars: the operator product expansions and the conformal invariance

The action in equation (10) consists of two massless scalars located in the 2D Euclidean space. Here, we summarize its basic properties, e.g., the equation of motion, the operator product expansions, and the conformal invariance [36].

It is convenient to adopt the complex coordinates $z, \bar{z} = x \pm \mathrm{i}y$ (the former takes the upper sign). When we define $\phi^\alpha(z, \bar{z}) \equiv \phi^\alpha(\mathbf{x}), \theta_\alpha(z, \bar{z}) \equiv \theta_\alpha(\mathbf{x}), \mathrm{d}^2 z \equiv 2\mathrm{d}^2 x$ and $\partial, \bar{\partial} \equiv (\partial_x \mp \mathrm{i}\partial_y)/2$, then equation (10) is expressed as

$$S_0 = \int \mathrm{d}^2 z \frac{K}{\pi} \partial\phi_\alpha(z, \bar{z}) \bar{\partial}\phi^\alpha(z, \bar{z}). \tag{A.1}$$

The classical equation of motion is then

$$\partial\bar{\partial}\phi^\alpha(z, \bar{z}) = 0, \tag{A.2}$$

which exhibits the chiral decomposition of fields, i.e.,

$$\phi^\alpha(z, \bar{z}), \theta^\alpha(z, \bar{z}) = \frac{K^{\mp\frac{1}{2}}}{2}[\psi^\alpha(z) \pm \bar{\psi}^\alpha(\bar{z})]. \tag{A.3}$$

In terms of new fields with only holomorphic or antiholomorphic dependence, the action is re-expressed as

$$S_0 = \int \mathrm{d}^2 z \frac{1}{4\pi} \partial\psi_\alpha(z) \bar{\partial}\bar{\psi}^\alpha(\bar{z}), \tag{A.4}$$

and their two-point functions are diagonal in the sense that

$$\langle \psi^\alpha(z)\psi^\beta(0)\rangle_0 = -g^{\alpha\beta} \ln \frac{z}{a}, \tag{A.5}$$

$$\langle \bar{\psi}^\alpha(\bar{z})\bar{\psi}^\beta(0)\rangle_0 = -g^{\alpha\beta} \ln \frac{\bar{z}}{a}, \tag{A.6}$$

which otherwise vanish. These show that ψ^α and $\bar{\psi}^\alpha$ are not the scaling operators. However, their derivatives

$$j^\alpha(z) \equiv \mathrm{i}a\partial\psi^\alpha(z) \qquad \text{and} \qquad \bar{j}^\alpha(\bar{z}) \equiv \mathrm{i}a\bar{\partial}\bar{\psi}^\alpha(\bar{z}) \tag{A.7}$$

exhibit, e.g., $\langle j^\alpha(z) j^\beta(0)\rangle_0 = g^{\alpha\beta}\,(a/z)^2$, so that j^α and $\bar{j}^\alpha$ are candidates of those with the scaling dimension 1. As usual, this issue can be confirmed by the OPE with the stress tensor which is obtained by the Noether theorem: it is diagonal in the complex coordinates, and is given by

$$T(z) = \tfrac{1}{2} : j_\alpha(z) j^\alpha(z) : \qquad \text{and} \qquad \overline{T}(\bar{z}) = \tfrac{1}{2} : \bar{j}_\alpha(\bar{z}) \bar{j}^\alpha(\bar{z}) : . \tag{A.8}$$

Using the Wick theorem and the Taylor expanding, the OPE's can be obtained as follows:

$$T(z) j^\alpha(0) \simeq \left(\frac{a}{z}\right)^2 j^\alpha(0) + \left(\frac{a}{z}\right)^1 a\partial j^\alpha(0), \tag{A.9}$$

$$\overline{T}(\bar{z}) \bar{j}^\alpha(0) \simeq \left(\frac{a}{\bar{z}}\right)^2 \bar{j}^\alpha(0) + \left(\frac{a}{\bar{z}}\right)^1 a\bar{\partial} \bar{j}^\alpha(0). \tag{A.10}$$

These exhibit that j^α and $\bar{j}^\alpha$ are the scaling operators with the conformal weights $(\Delta, \overline{\Delta}) = (1, 0)$ and $(0, 1)$, respectively. The vertex operators are also important examples of the scaling operators; they are introduced by

$$v_{\mathbf{k}}(z) \equiv : \mathrm{e}^{\mathrm{i}k_\alpha \psi^\alpha(z)} : \qquad \text{and} \qquad \bar{v}_{\bar{\mathbf{k}}}(\bar{z}) \equiv : \mathrm{e}^{\mathrm{i}\bar{k}_\alpha \bar{\psi}^\alpha(\bar{z})} : . \tag{A.11}$$

The two-point functions behave as, e.g., $\langle v_{\mathbf{k}}(z) v_{-\mathbf{k}}(0)\rangle_0 = (a/z)^{\|\mathbf{k}\|^2}$, where k_α is the covariant element of a constant vector $\mathbf{k}$ and $\|\mathbf{k}\|^2 \equiv k_\alpha k^\alpha$. Similarly to the above, the OPE's of Tv and $\overline{T}\bar{v}$ are given as follows:

$$T(z) v_{\mathbf{k}}(0) \simeq \frac{\|\mathbf{k}\|^2}{2} \left(\frac{a}{z}\right)^2 v_{\mathbf{k}}(0) + \left(\frac{a}{z}\right)^1 a\partial v_{\mathbf{k}}(0), \tag{A.12}$$

$$\overline{T}(\bar{z}) \bar{v}_{\bar{\mathbf{k}}}(0) \simeq \frac{\|\bar{\mathbf{k}}\|^2}{2} \left(\frac{a}{\bar{z}}\right)^2 \bar{v}_{\bar{\mathbf{k}}}(0) + \left(\frac{a}{\bar{z}}\right)^1 a\bar{\partial} \bar{v}_{\bar{\mathbf{k}}}(0). \tag{A.13}$$

Thus, $v_{\mathbf{k}}$ and $\bar{v}_{\bar{\mathbf{k}}}$ are the scaling operators with the weights $(\|\mathbf{k}\|^2/2, 0)$ and $(0, \|\bar{\mathbf{k}}\|^2/2)$, respectively.

As we have seen, although the physical quantities possess both the holomorphic and the antiholomorphic parts, the OPE's are performed independently in these two parts due to the diagonal nature of the two-point functions (A.5) and (A.6). Therefore, for a while, we focus only on the holomorphic part. The OPE of T with itself is given by

$$T(z) T(0) \simeq \frac{\delta^\alpha_\alpha}{2} \left(\frac{a}{z}\right)^4 + 2\left(\frac{a}{z}\right)^2 T(0) + \left(\frac{a}{z}\right)^1 a\partial T(0). \tag{A.14}$$

Thus, we can read off the central charge as $c = \delta^\alpha_\alpha = 2$, which is equal to the number of components of the vector field. The OPE between j_α and $v_{\mathbf{k}}$ are given by

$$j_\alpha(z) v_{\mathbf{k}}(0) \simeq k_\alpha \left(\frac{a}{z}\right)^1 v_{\mathbf{k}}(0). \tag{A.15}$$

This indicates that j_α is the current operator to detect the αth element of the vector charge $\mathbf{k}$ in the vertex operator. Further, the OPE between two vertex operators plays a very important role in our discussion; it can be expressed in the following form:

$$v_{\mathbf{k}}(z) v_{-\mathbf{k}'}(0) \simeq \left(\frac{a}{z}\right)^{\mathbf{k}\cdot\mathbf{k}'} : v_{\mathbf{k}-\mathbf{k}'}(0) \left[1 + \mathrm{O}\left(\frac{z}{a}\right)\right] : . \tag{A.16}$$

For the case $\mathbf{k} \neq \mathbf{k}'$, we can neglect the $\mathrm{O}(z/a)$ terms in the rhs. However, for $\mathbf{k} = \mathbf{k}'$, since $v_{\mathbf{0}}(z) = \hat{1}$ by definition, they become important. By expansion, we find

$$\frac{z}{a} k_\alpha j^\alpha(0) + \frac{1}{2}\left(\frac{z}{a}\right)^2 \{k_\alpha a \partial j^\alpha(0) + [k_\alpha j^\alpha(0)]^2\}, \tag{A.17}$$

where the $\mathrm{O}((z/a)^3)$ terms are dropped.

Appendix B. Some useful relations

In this appendix, we shall derive some useful relations which will be referred to in the discussion of section 2. Using equation (A.7), the $\mathcal{M}$ operator in equation (14) is given by

$$\mathcal{M}(\mathbf{x}) = -\tfrac{1}{\sqrt{2}} j_\alpha(z) \bar{j}^\alpha(\bar{z}). \tag{B.1}$$

On the other hand, using equation (A.11), the vertex operator with the vector charges, $\mathbf{M}$ and $\mathbf{N}$, is expressed as

$$: \mathrm{e}^{\mathrm{i}[\mathbf{M}\cdot\boldsymbol{\Phi}(\mathbf{x}) + \mathbf{N}\cdot\boldsymbol{\Theta}(\mathbf{x})]} := v_{\mathbf{K}}(z) \bar{v}_{\overline{\mathbf{K}}}(\bar{z}) \tag{B.2}$$

with $\mathbf{K}$, $\overline{\mathbf{K}} \equiv (K^{-\frac{1}{2}}\mathbf{M} \mp K^{+\frac{1}{2}}\mathbf{N})/\sqrt{2}$. From equations (A.12) and (A.13), we can obtain the formula for the scaling dimension of the vertex operator, $x_{\mathbf{M},\mathbf{N}} = \frac{1}{2}(\|\mathbf{K}\|^2 + \|\overline{\mathbf{K}}\|^2)$. It is rewritten as a function of the vectors

$$x_{\mathbf{M},\mathbf{N}} = \tfrac{1}{2}(K^{-1}\|\mathbf{M}\|^2 + K\|\mathbf{N}\|^2). \tag{B.3}$$

The OPE between the $\mathcal{M}$ operator and the vertex operator is calculated by using equation (A.15) as

$$\mathcal{M}(\mathbf{x}) : \mathrm{e}^{\mathrm{i}[\mathbf{M}\cdot\boldsymbol{\Phi}(\mathbf{0}) + \mathbf{N}\cdot\boldsymbol{\Theta}(\mathbf{0})]} :\simeq -\frac{\mathbf{K}\cdot\overline{\mathbf{K}}}{\sqrt{2}} \left|\frac{a}{z}\right|^2 : \mathrm{e}^{\mathrm{i}[\mathbf{M}\cdot\boldsymbol{\Phi}(\mathbf{0}) + \mathbf{N}\cdot\boldsymbol{\Theta}(\mathbf{0})]} :, \tag{B.4}$$

where the coefficient is also given by $\mathbf{K}\cdot\overline{\mathbf{K}} = x_{\mathbf{M},\mathbf{0}} - x_{\mathbf{0},\mathbf{N}}$.

The OPE's between the vertex operators with opposite vector charges are the most important part in our calculations. Here, we consider the following quantity:

$$\mathcal{Q} \equiv \frac{1}{6} \sum_{\|\mathbf{M}\| = pa^*} : \mathrm{e}^{\mathrm{i}\mathbf{M}\cdot\boldsymbol{\Phi}(\mathbf{x})} :: \mathrm{e}^{-\mathrm{i}\mathbf{M}\cdot\boldsymbol{\Phi}(\mathbf{0})} :, \tag{B.5}$$

where the summation is over the six vectors in equation (12). The product of the holomorphic and the antiholomorphic parts gives many terms. Among them, those of the first order in the elements of the vector charge $\mathbf{M}$ disappear after the summation. For the second-order terms, by utilizing the relation,

$$\frac{1}{6} \sum_{\|\mathbf{M}\| = pa^*} m_\alpha m_\beta = \frac{2p^2}{3} g_{\alpha\beta}, \tag{B.6}$$

we find the following compact expression:

$$\mathcal{Q} \simeq \left|\frac{a}{z}\right|^{4p^2/3K} \left\{1 + \frac{p^2}{3K}\left[\left(\frac{z}{a}\right)^2 T(0) + \left(\frac{\bar{z}}{a}\right)^2 \overline{T}(0) - \left|\frac{z}{a}\right|^2 \sqrt{2}\mathcal{M}(\mathbf{0})\right]\right\}. \tag{B.7}$$

Similarly, we can perform the OPE calculation of the following quantity

$$\mathcal{R} \equiv \frac{1}{6} \sum_{\|\mathbf{N}\| = 1} : \mathrm{e}^{\mathrm{i}\mathbf{N}\cdot\boldsymbol{\Theta}(\mathbf{x})} :: \mathrm{e}^{-\mathrm{i}\mathbf{N}\cdot\boldsymbol{\Theta}(\mathbf{0})} :, \tag{B.8}$$

where the summation is over the six vectors given in equation (13). Like equation (B.6), the relation between the elements of the vector charge **N** and the metric tensor,

$$\frac{1}{6}\sum_{\|\mathbf{N}\|=1} n^{\alpha}n^{\beta} = \frac{1}{2}g^{\alpha\beta}, \tag{B.9}$$

is available. So, one can find the expansion

$$\mathcal{R} \simeq \left|\frac{a}{z}\right|^{K}\left\{1+\frac{K}{4}\left[\left(\frac{z}{a}\right)^{2}T(0)+\left(\frac{\bar{z}}{a}\right)^{2}\overline{T}(0)+\left|\frac{z}{a}\right|^{2}\sqrt{2}\mathcal{M}(\mathbf{0})\right]\right\}. \tag{B.10}$$

Consequently, we see that the OPE's include the secondary operators T with $(\Delta, \overline{\Delta}) = (2, 0)$ and $\overline{T}$ with (0, 2) as well as the $\mathcal{M}$ operator with (1, 1) (see also [68]). In general, a rotationally invariant system defined on the plain does not include T and $\overline{T}$ because they possess the conformal spins with length 2. On the other hand, since the $\mathcal{M}$ operator is scalar and proportional to $\mathcal{L}_0$, these results naturally exhibit the renormalizations of the Gaussian coupling K caused by the potentials $\mathcal{L}_{1,2}$, and may also indicate that the metric tensor has been properly employed to define the fixed-point Lagrangian density $\mathcal{L}_0$.

References

[1] Belavin A A, Polyakov A M and Zamolodchikov A B 1984 *Nucl. Phys.* B **241** 333
[2] Friedan D, Qiu Z and Shenker S 1984 *Phys. Rev. Lett.* **52** 1575
[3] Wannier G H 1950 *Phys. Rev.* **79** 357
Wannier G H 1973 *Phys. Rev.* B **7** 5017
[4] Houtapple R M F 1950 *Physica* **16** 425
[5] Husimi K and Syozi I 1950 *Prog. Theor. Phys.* **5** 177
Syozi I 1950 *Prog. Theor. Phys.* **5** 341
[6] Stephenson J 1970 *J. Math. Phys.* **11** 413
[7] Lieb E H 1967 *Phys. Rev.* **162** 162
Lieb E H 1967 *Phys. Rev. Lett.* **18** 692
[8] Baxter R J 1970 *J. Math. Phys.* **11** 3116
Baxter R J 1982 *Proc. R. Soc.* A **383** 43
[9] Baxter R J 1970 *J. Math. Phys.* **11** 784
[10] Huse D A and Rutenberg A D 1992 *Phys. Rev.* B **45** R7536
[11] Lieb E H and Wu F Y 1972 *Phase Transitions and Critical Phenomena* vol 1 ed C Domb and M S Green (London: Academic)
[12] Read N Unpublished
[13] Kondev J and Henley C L 1995 *Phys. Rev.* B **52** 6628
[14] Kondev J and Henley C L 1996 *Nucl. Phys.* B **464** 540
[15] For instance, see Ghosh A, Dhar D and Jacobsen J L 2007 *Phys. Rev.* E **75** 011115
[16] Thijssen J M and Knops H J F 1990 *Phys. Rev.* B **42** 2438
[17] Baxter R J and Wu F Y 1973 *Phys. Rev. Lett.* **31** 1294
[18] Alcaraz F C and Xavier J C 1999 *J. Phys. A: Math. Gen.* **32** 2041
[19] Alcaraz F C and Jacobs L 1982 *J. Phys. A: Math. Gen.* **15** L357
[20] Alcaraz F C, Cardy J L and Ostlund S 1983 *J. Phys. A: Math. Gen.* **16** 159
[21] José J V, Kadanoff L P, Kirkpatrick S and Nelson D R 1977 *Phys. Rev.* B **16** 1217
[22] Kosterlitz J M and Thouless J D 1973 *J. Phys. C: Solid State Phys.* **6** 1181
[23] Halperin B I and Nelson D R 1978 *Phys. Rev. Lett.* **41** 121
[24] Nelson D R and Halperin B I 1979 *Phys. Rev.* B **19** 2457
[25] Young A P 1979 *Phys. Rev.* B **19** 1855
[26] Nelson D R 1978 *Phys. Rev.* B **18** 2318
[27] For recent application, see Jacobsen J L and Kondev J 2004 *Phys. Rev.* E **69** 066108
Jacobsen J L and Kondev J 2004 *Phys. Rev. Lett.* **92** 210601
[28] Otsuka H 2007 *J. Phys. Soc. Japan* **76** 073002
[29] Nomura K 1995 *J. Phys. A: Math. Gen.* **28** 5451

[30] Berezinskii V L 1971 *Pis'ma Zh. Eksp. Teor. Fiz.* **61** 1144
Berezinskii V L 1972 *JETP* **34** 610
[31] Kosterlitz J M 1974 *J. Phys. C: Solid State Phys.* **7** 1046
[32] Matsuo H and Nomura K 2006 *J. Phys. A: Math. Gen.* **39** 2953
[33] Otsuka H, Mori K, Okabe Y and Nomura K 2005 *Phys. Rev.* E **72** 046103
[34] Otsuka H, Okabe Y and Okunishi K 2006 *Phys. Rev.* E **73** 035105
[35] Otsuka H, Okabe Y and Nomura K 2006 *Phys. Rev.* E **74** 011104
[36] Polchinski J 1998 *String Theory* vol 1 (England: Cambridge University Press)
[37] Kadanoff L P 1979 *Ann. Phys.* **120** 39
[38] Kadanoff L P and Brown A C 1979 *Ann. Phys.* **121** 318
[39] Polyakov A M 1972 *Zh. Eksp. Teor. Fiz.* **63** 24
Polyakov A M 1973 *Sov. Phys.—JETP* **36** 12
[40] Houghton A and Ogilvie M C 1980 *J. Phys. A: Math. Gen.* **13** L449
[41] Boyanovsky D and Holman R 1991 *Nucl. Phys.* B **358** 619
[42] Giamarchi T and Schulz H J 1989 *Phys. Rev.* B **39** 4620
[43] Cardy J L 1986 *J. Phys. A: Math. Gen.* **19** L1093
[44] Cardy J L 1984 *J. Phys. A: Math. Gen.* **17** L385
[45] Blöte H W J, Cardy J L and Nightingale M P 1986 *Phys. Rev. Lett.* **56** 742
[46] Affleck I 1986 *Phys. Rev. Lett.* **56** 746
[47] Otsuka H 2008 *Phys. Rev.* E **77** 062101
[48] Fisher M E, Barber M N and Jasnow D 1973 *Phys. Rev.* A **8** 1111
[49] Nelson D R and Kosterlitz J M 1977 *Phys. Rev. Lett.* **39** 1201
[50] Ohta T and Jasnow D 1979 *Phys. Rev.* B **20** 139
[51] Uimin G V 1970 *Pisma Zh. Eksp. Teor. Fiz.* **12** 332
Uimin G V 1970 *JETP Lett.* **12** 225
[52] Lai C K 1974 *J. Math. Phys.* **15** 1675
[53] Sutherland B 1975 *Phys. Rev.* B **12** 3795
[54] Affleck I, Kennedy T, Lieb E H and Tasaki H 1987 *Phys. Rev. Lett.* **59** 799
[55] Takhtajan L A 1982 *Phys. Lett.* A **87** 479
[56] Babujian H M 1982 *Phys. Lett.* A **90** 479
Babujian H M 1983 *Nucl. Phys.* B **215** 317
[57] Fath G and Solyom J 1991 *Phys. Rev.* B **44** 11836
[58] Fath G and Solyom J 1993 *Phys. Rev.* B **47** 872
[59] Haldane F D M 1983 *Phys. Lett.* A **93** 464
Haldane F D M 1983 *Phys. Rev. Lett.* **50** 1153
[60] Itoi C and Kato M 1997 *Phys. Rev.* B **55** 8295
[61] Hijii K 2006 Private communication
[62] Lecheminant P and Totsuka K 2006 *J. Stat. Mech.* L12001
[63] Lecheminant P 2007 *Phys. Lett.* B **648** 323
[64] Frenkel I B and Kac V G 1980 *Invent. Math.* **62** 23
[65] Segal G 1981 *Commun. Math. Phys.* **80** 301
[66] Peczak P and Landau D P 1989 *Phys. Rev.* B **39** 11932
[67] Lee J and Kosterlitz J M 1990 *Phys. Rev. Lett.* **65** 137
[68] Kadanoff L P 2000 *Statistical Physics, Statics, Dynamics and Renormalization* (Singapore: World Scientific)